energies

MDPI

Article

Dandelion-Root Extract as Green Corrosion Inhibitor for Carbon Steel in CO_2-Saturated Brine Solution

Katarina Žbulj, Lidia Hrnčević *, Gordana Bilić and Katarina Simon

Faculty of Mining, Geology and Petroleum Engineering, University of Zagreb, 10000 Zagreb, Croatia; katarina.zbulj@rgn.unizg.hr (K.Ž.); gordana.bilic@rgn.unizg.hr (G.B.); katarina.simon@rgn.unizg.hr (K.S.)
* Correspondence: lidia.hrncevic@rgn.unizg.hr

Abstract: Recently, due to the corrosion problem in the petroleum industry and the usage of commercial corrosion inhibitors, which, when released untreated into the environment, are considered to be environmentally unfriendly, green corrosion inhibitors are being researched. In this paper, the results of dandelion-root-extract testing as a green corrosion inhibitor for carbon steel in simulated brine solution saturated with carbon dioxide (CO_2) are shown. The extract's inhibition efficiency in static and flow conditions was determined by using potentiodynamic polarization with Tafel extrapolation and electrochemical-impedance-spectroscopy methods. In static conditions, the extract was tested at different concentrations. A maximum inhibition efficiency of 98.37% in static conditions at an extract concentration of 12 mL/L and 82.80% in flow conditions at a concentration of 14 mL/L was achieved. Additionally, for the most efficient dandelion-root-extract concentration (12 mL/L), the biodegradability and toxicity were determined. A biodegradability of 0.96 and a toxicity of 2.38% was achieved. Based on the obtained results of the conducted laboratory measurements, it can be concluded that dandelion-root extract has significant potential in terms of its use as a green corrosion inhibitor for carbon steel in a CO_2-saturated brine solution.

Keywords: dandelion-root extract; green corrosion inhibitor; carbon steel; CO_2-saturated brine solution

Citation: Žbulj, K.; Hrnčević, L.; Bilić, G.; Simon, K. Dandelion-Root Extract as Green Corrosion Inhibitor for Carbon Steel in CO_2-Saturated Brine Solution. *Energies* **2022**, *15*, 3074. https://doi.org/10.3390/en15093074

Academic Editor: Hossein Hamidi

Received: 31 March 2022
Accepted: 20 April 2022
Published: 22 April 2022

1. Introduction

From its very beginning, corrosion has posed a serious and complex problem for the petroleum industry and as such, requires a detailed analysis and a systematic management approach. On one hand, most of the pipelines and equipment in the petroleum industry are made of carbon steel, which, under certain conditions and in specific (corrosive) environments, is subject to corrosion. On the other hand, the petroleum industry deals with fluids that are susceptible to the formation of a corrosive environment. During hydrocarbon production, depending on the type of reservoir, there is always a certain amount of brine produced, with the quantities increasing as the production field matures. Along with brine (containing a significant amount of salt), the production fluid also contains some other impurities such as carbon dioxide (CO_2) and hydrogen sulfide (H_2S), which create highly corrosive environments.

The fluid flow has a great influence on the corrosion rate and surface processes. When a protective ferrous-carbonate ($FeCO_3$) layer is formed or an inhibitor film covers the steel surface, the effect of flow becomes meaningless because in that case, the main corrosion resistance is that layer/inhibitor film. On the other hand, turbulent flow could interfere with the forming of the mentioned protective ferrous-carbonate ($FeCO_3$) layer/inhibitor film, or it could mechanically damage it, which can lead to greater risk of localized corrosion attack [1].

Corrosion damages equipment, reduces infrastructure lifetime, has potentially harmful effects on the environment, and consequently causes high costs. The total costs of corrosion in the oil and gas production industry have been estimated to be 1.372×10^9 US dollars

per year, of which the highest share is attributed to the costs of the corrosion of surface facilities (pipelines and surface processing equipment) (43%) and downhole equipment (tubing) (34%) [2]. According to the latest report of the National Association of Corrosion Engineers (NACE), the *International Measures and Prevention*, *Application and Economics of Corrosion Technologies* (the IMPACT report), the global corrosion costs have been estimated to 2.5×10^{18} US dollars, which, in 2016 when the IMPACT report was issued, was equivalent to 3.4% of the global Gross Domestic Product (GDP) [3]. Although the corrosion problem in the petroleum industry cannot be fully avoided, this problem can be mitigated, among others, by the application of corrosion inhibitors. Since commonly used, conventional corrosion inhibitors (usually organic inhibitors with polar functional groups, such as pyridines, imidazolines or amides [4,5] containing sulphur (S), phosphorus (P), oxygen (O) and nitrogen (N) atoms) are considered to be harmful to the environment, there is a strong initiative aimed at developing equally effective, less toxic and biodegradable so-called green corrosion inhibitors. There are several groups of compounds that are considered to be green corrosion inhibitors, such as medicaments, amino acids, biopolymers, Rare Earth elements, and plant extracts [6–8]. Out of the stated green corrosion inhibitors, due to their non-toxic and biodegradable nature and simple and economical extraction process, nowadays, most research has been performed using plant extracts. The extracts of many plants have been considered to be green corrosion inhibitors [9].

Most of the plants' extracts considered to be green corrosion inhibitors have been tested in acidic environments (HCl, H_2SO_4, H_2CO_3) [10–19] with fewer being tested in neutral media [20–22]. As mentioned before, in the oil and gas production system, inner corrosion mostly occurs because of the formation of a salty-acid environment due to sour gas dissolution in brine, so, in order to test green corrosion inhibitors' efficiency for such systems, the initial tests should at least be performed in brine saturated with CO_2.

In the selection phase, ten plants were tested [23]. The results of the preliminary tests pointed to dandelion-root extract as a potential corrosion inhibitor in brine solution saturated with CO_2. In this paper, the results of the inhibitor efficiency of dandelion-root extract in static and flow conditions, determined through electrochemical methods (Tafel polarization and electrochemical-impedance spectroscopy (EIS)), are presented. Additionally, the results of scanning electron microscopy (SEM) and Fourier-transform infrared spectroscopy (FTIR), which were conducted to determine how the inhibitor is adsorbed on a steel surface and through which active groups, are shown. Lastly, the biodegradability and toxicity of the extract were determined.

2. Materials and Methods

In this study, dandelion-root extract was tested as a green corrosion inhibitor for carbon steel in brine saturated with CO_2. The inhibitor efficiency was tested in static and flow conditions by using electrochemical methods (Tafel polarization and EIS). The chemical composition of the carbon-steel sample is shown in Table 1. The composition was determined by optical emission spectrometry on spectrophotometer GDS 850 A, LECO. Before each measurement, the carbon-steel sample was polished with 300, 600 and 1200 grit abrasive paper, then washed with distilled water and finally degreased with ethanol (96%). The carbon-steel-sample area exposed to the solution was 1 cm^2.

Table 1. Chemical composition of carbon steel (wt. %) [23].

C	Si	Mn	P	S	Cr	Mo	Ni	Cu	Fe
0.32	0.25	1.38	0.016	0.009	0.24	<0.01	0.02	0.01	balance

The solution that served as a corrosive media was a simulated brine solution with or without the added dandelion-root extract. The chemical composition of the simulated brine solution is shown in Table 2. Prior to the tests, the solution was firstly saturated with carbon dioxide for 45 min, followed by continuous saturation during the measurement.

Commercially available liquid dandelion-root extract (with 80% flavonoids), Soria Natural, Spain, was used for these measurements. Dandelion-root extract was added at concentrations ranging from 10 mL/L to 13 mL/L with a concentration increase of 1 mL/L per measurement for static conditions. For flow conditions, the tested concentration range of dandelion-root extract was from 11 mL/L to 15 mL/L with an increase of 1 mL/L per measurement. The concentration range was selected based on the available literature on the previously conducted research on dandelion-root extract and the results of the self-performed preliminary research [23].

Table 2. Chemical composition of the simulated brine solution [23].

Chemical Compound	γ (g/L)
NaCl	30.0
$NaHCO_3$	0.1
$CaCO_3$	0.1

The measurements were conducted by using a three-electrode corrosion cell, as shown in Figure 1. After immersing a carbon-steel sample into the solution, the electrode was stabilized for 1 h before performing electrochemical measurements. All measurements were performed at ambient temperature. As a counter electrode, for measurement in static conditions, two graphite rods were used, and for measurement in flow conditions, a platinum electrode was used. As a reference electrode for measurements in both conditions, a saturated calomel electrode (SCE) was used. In flow conditions, measurements were conducted under a maximum flow of 50 cm^3/min, which is equivalent to a maximum flow rate of 400 cm/min for this flow cell. This flow rate is achieved in real field conditions in flowlines in the case of a flow of approximately 20 m^3/d. Electrochemical measurements were performed using SP1 Potentiostat and SmartManager software with IVMAN and ZMAN programs used to analyze data. All measurements were performed three times for better data reproducibility. Very good reproducibility was achieved with less than 5% of relative standard deviation.

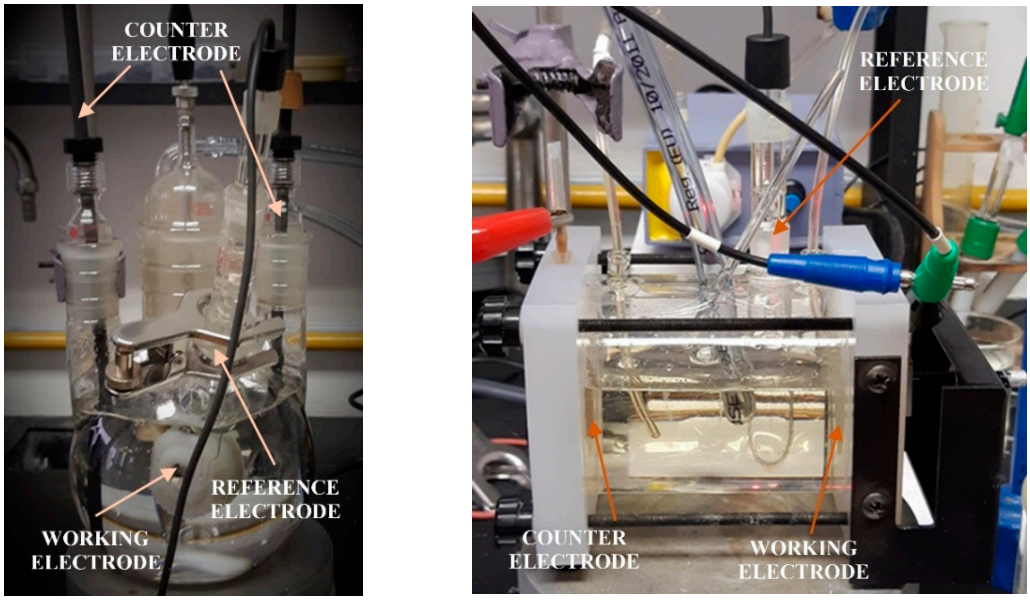

(**a**) (**b**)

Figure 1. Three-electrode corrosion cell (**a**) for static conditions (Adapted from [23]); (**b**) for flow conditions (Adapted from [24]).

For potentiodynamic polarization with Tafel extrapolation, the corrosion potential was set to ±250 mV versus open circuit potential after stabilizing the electrode for 1 h,

with a scan rate of 0.166 mV/s. Using this method, the corrosion rate and inhibition efficiency were determined. Electrochemical-impedance spectroscopy was performed in a frequency range from 100 kHz to 1 mHz. Some of the EIS measurements were stopped before reaching the frequency of 1 mHz, which in the case of our measurements did not affect the results nor the selected equivalent electrical circuits. Characterization of a steel surface with or without an inhibitor was conducted through the nondestructive EIS method. Besides electrochemical measurements, the surface-examination methods of SEM and FTIR were used to determine the mechanism of the inhibitor adsorption on the metal surface. The morphology of the steel surface was observed using a TESCAN VEGA TS5136LS scanning electron microscope and FTIR spectra were recorded in Fourier-transform infrared Spectrum One, Perkin Elmer spectrophotometer (Great Britain), which extended from 650 cm^{-1} to 4000 cm^{-1}. Both surface-examination methods were performed with carbon-steel samples that had been immersed for a period of four hours in the brine solution to which the inhibitor (dandelion-root extract) was added at the most effective concentration and compared with the pure liquid extract. To determine the environmental impact of the inhibitor, the biodegradability and toxicity of dandelion-root extract was examined. The value of chemical oxygen demand (COD) was spectrophotometrically determined at 670 nm (Hach model DR/2400), while biological oxygen demand (BOD) was determined by Winkler's method. For the determination of toxicity, bioluminescent bacteria *Vibrio fischeri* and luminometer LUMIStox 300 (Dr Lange GmbH, Germany) were used.

3. Results and Discussion

3.1. Electrochemical Measurements

3.1.1. Polarization Curves

To examine dandelion-root extract corrosion-inhibition efficiency, measurements of potentiodynamic polarization were performed. The scanned polarization curves for the measurements in static conditions are shown in Figure 2. Electrochemical parameters, such as corrosion potential (E_{corr}), corrosion current (j_{corr}), anodic and cathodic Tafel slopes (β_a, β_c respectively), corrosion rate (v_{corr}) and inhibitor efficiency (IE) determined from polarization curves are shown in Table 3. The inhibitor efficiency was calculated from Equation (1) [25] as follows:

$$IE(\%) = \frac{v_{corr}^{0} - v_{corr}^{inh}}{v_{corr}^{0}} \times 100 \quad (1)$$

where IE is the inhibitor efficiency (%), and v_{corr}^{0} and v_{corr}^{inh} represent the corrosion rate (mm/year) in solution with and without an inhibitor.

Table 3. Electrochemical parameters determined from polarization curves scanned on the carbon-steel sample in the simulated brine saturated with CO_2 with and without inhibitor in static conditions (Data from [24]).

γ (mL/L)	0	10	11	12	13
E_{corr} (mV)	−741	−712	−716	−681	−703
j_{corr} (μA/cm^2)	97.627	23.240	7.788	1.594	5.431
$-\beta_c$ (V/dec)	0.517	0.438	0.358	0.261	0.297
β_a (V/dec)	0.065	0.062	0.057	0.065	0.066
v_{corr} (mm/year)	1.136	0.271	0.091	0.019	0.063
IE (%)	-	76.19	92.02	98.37	94.44

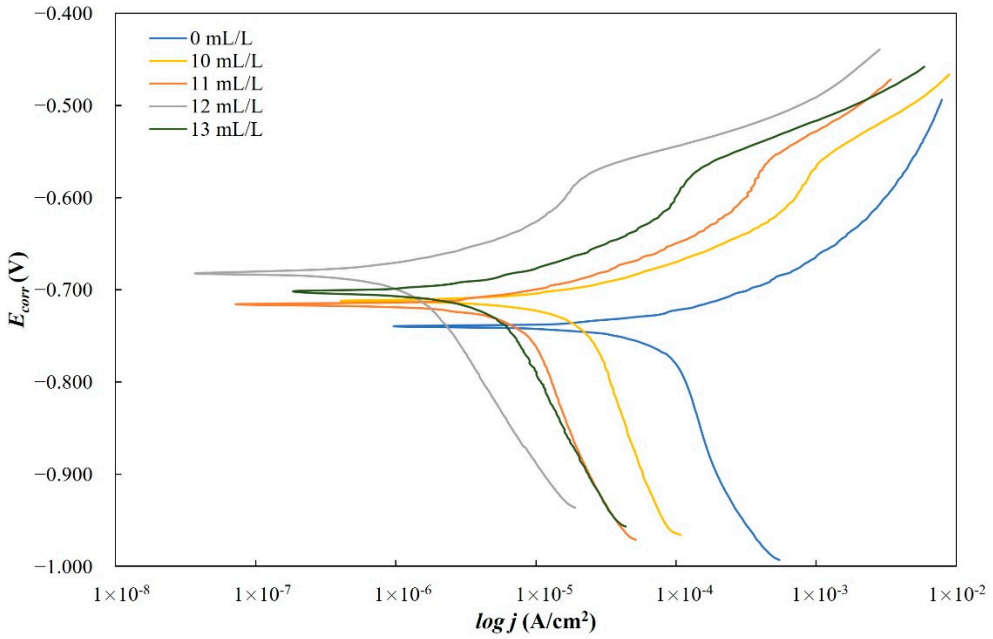

Figure 2. Polarization curves scanned on the carbon-steel sample in the simulated brine saturated with CO_2 with and without an inhibitor in static conditions (Adapted from [24]).

From Figure 2, it can be seen that at every concentration, both anodic and cathodic polarization curves are suppressed via lower values of corrosion current, which can indicate a slower anodic and cathodic corrosion process. Additionally, at the anodic part of the curve at approximately −575 mV, a depassivation potential can be seen, which can imply the formation of a passive film on the metal surface, at which point it loses its protective properties [26]. At the highest inhibitor concentration, the micelles are forming, i.e., the critical micelle concentration of the inhibitor is achieved, which causes the inhibitor efficiency to decrease. Due to the values of corrosion potential becoming more positive and the lower slope of the cathodic line, it can be concluded that the dandelion-root extract behaves as a mixed type of inhibitor for carbon-steel corrosion in simulated brine saturated with CO_2 in static conditions. It can be seen in Table 3 that an increase in inhibitor concentration results in a decrease in corrosion rate and an increase in inhibitor efficiency, indicating that dandelion-root extract protects carbon steel from corrosion in simulated brine saturated with CO_2 in static conditions. The highest inhibitor efficiency (98.37%) was achieved at an inhibitor concentration of 12 mL/L.

Polarization curves of measurements conducted in flow conditions are shown in Figure 3, and Table 4 gives the polarization parameters determined from the curves.

Table 4. Electrochemical parameters determined from polarization curves scanned on the carbon-steel sample in the simulated brine saturated with CO_2 with and without inhibitor in flow conditions (Data from [24]).

γ (mL/L)	0	11	12	13	14	15
E_{corr} (mV)	−599	−684	−710	−718	−724	−587
j_{corr} (μA/cm^2)	231.056	99.020	73.787	64.314	39.743	53.513
$-\beta_c$ (V/dec)	1.492	0.909	0.452	0.533	0.369	0.344
β_a (V/dec)	0.125	0.092	0.090	0.117	0.108	0.079
v_{corr} (mm/year)	2.689	1.152	0.859	0.749	0.463	0.623
IE (%)	-	57.16	68.07	72.17	82.80	76.84

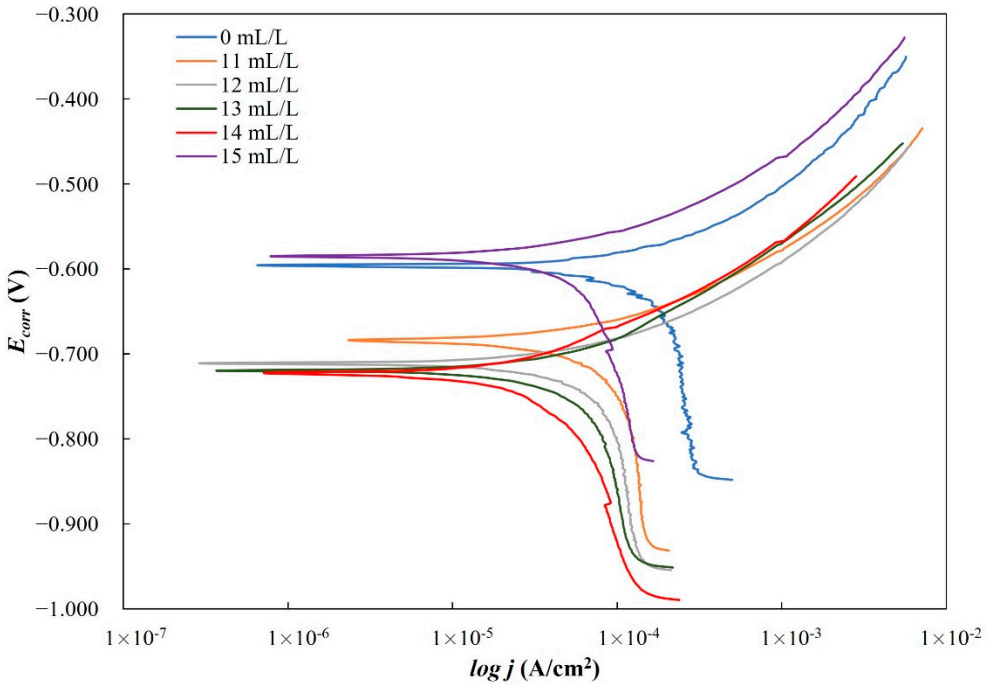

Figure 3. Polarization curves scanned on the carbon-steel sample in the simulated brine saturated with CO_2 with and without inhibitor in flow conditions (Adapted from [24]).

With an increase in the inhibitor concentration, the corrosion potential moves towards more negative values, except at the inhibitor concentration of 15 mL/L, as can be seen in Figure 3. Additionally, anodic and cathodic slopes are decreasing, which can also be seen in Table 4. Due to such behavior, it can be concluded that dandelion-root extract acts as a mixed-type inhibitor for carbon-steel corrosion in simulated brine saturated with CO_2 in flow conditions. Due to the concentration increase, the inhibitor efficiency also increases (Table 4), which indicates that dandelion-root extract protects carbon steel even in flow conditions. At the inhibitor concentration of 14 mL/L, the highest inhibitor efficiency of 82.8% was achieved.

3.1.2. Electrochemical-Impedance Spectroscopy

For the analysis of experimental data, two equivalent electrical circuits were used. For the uninhibited solutions and the solution containing 10 mL/L of the extract in static, and 11 mL/L of the extract in flow conditions, the circuit shown in Figure 4a was used. For all the other concentrations (11–13 mL/L in static, 12–15 mL/L in flow conditions) the circuit shown in Figure 4b was used. In those equivalent circuits, R_{el} represents the solution resistance, R_p is the charge-transfer resistance and R_{po} is the resistance of the inhibitor film pores. *CPE* represents the constant phase elements that were used instead of a capacitor because of the non-homogenic system. The *CPE* includes capacity Q and the deviation from the ideal behavior n. CPE_{dl} is the constant phase element that describes the capacitance of a double layer and CPE_{inh} describes the capacitance of the inhibitor film. The relation between capacitor (C) and the constant phase element (*CPE*) is defined by Equation (2) [27] where j is the current, and ω the angular frequency:

$$j \times \omega \times C = (j \times \omega)^n \times CPE \quad (2)$$

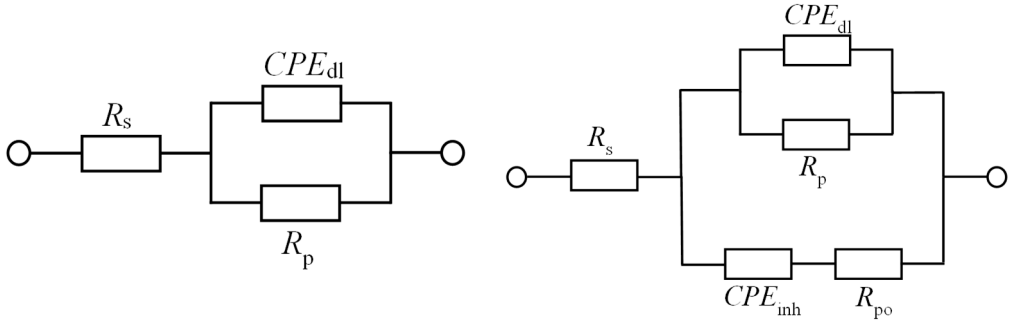

Figure 4. (**a**) Simple equivalent circuit (**b**) Equivalent circuit for the inhibited solution (Adapted from [24]).

The results of electrochemical-impedance spectroscopy (EIS) scanned on the carbon-steel sample immersed into the simulated brine saturated with CO_2 with and without the inhibitor in static conditions can be seen in Figures 5 and 6.

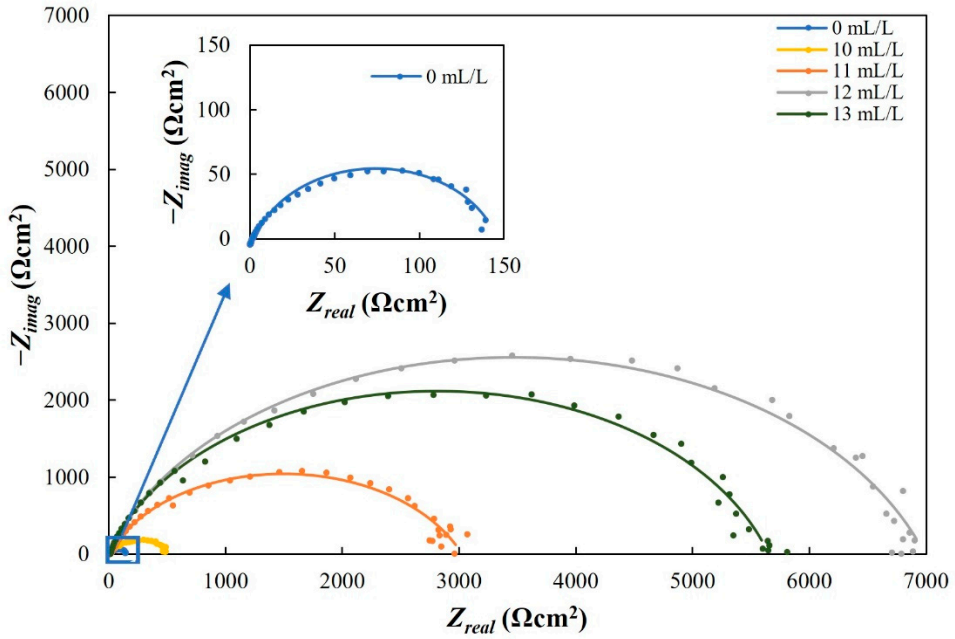

Figure 5. Nyquist plot scanned on the carbon-steel sample in the simulated brine saturated with CO_2 with and without the inhibitor in static conditions (Adapted from [24]).

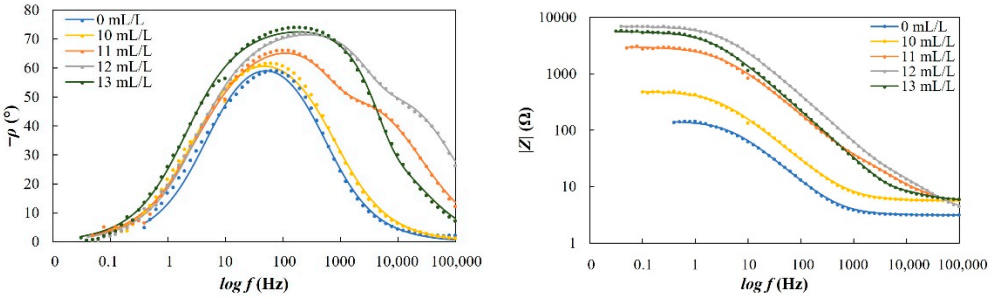

Figure 6. Bode plots scanned on the carbon-steel sample in the simulated brine saturated with CO_2 with and without the inhibitor in static conditions (Adapted from [24]).

The results of the adjustment of the experimental data with the equivalent circuit using ZMAN program are shown in Table 5. The inhibitor efficiency was calculated according to Equation (3) [14,28]:

$$IE(\%) = \frac{R_p^{inh} - R_p^0}{R_p^{inh}} \times 100 \quad (3)$$

where R_p^{inh} (Ω) and R_p^0 (Ω) represent charge-transfer resistance in the inhibited and the uninhibited solution.

Table 5. Electrochemical parameters determined from Nyquist and Bode plots scanned on the carbon-steel sample in the simulated brine saturated with CO_2 with and without the inhibitor in static conditions (Adapted from [24]).

γ (mL/L)	0	10	11	12	13
R_{el} (Ω)	3.12	5.62	4.96	3.24	5.56
Q_{dl} ($\mu\Omega^{-1}$ s^n)	410	210	34	12.2	22.3
n_1	0.83	0.80	0.74	0.78	0.81
R_p (Ω)	142.78	487.96	3022.56	6985.15	5650.19
Q_{inh} ($\mu\Omega^{-1}$ s^n)	-	-	2.23	0.82	0.26
n_2	-	-	0.98	0.99	1.15
R_{po} (Ω)	-	-	105.79	52.69	15.47
IE (%)		70.74	95.28	97.96	97.47

From the Nyquist plot (Figure 5) it can be seen that the increase in inhibitor concentration causes an increase in the diameter of semicircles. Additionally, the Bode plots (Figure 6) show the increase in impedance module and phase angle which can indicate adsorption of the inhibitor on the metal surface. An increase in the inhibitor concentration leads to an increase in the charge-transfer resistance (Table 5). It can be seen that the inhibitor efficiency also increases. At the inhibitor concentration of 12 mL/L, the highest efficiency of the inhibitor (97.96%) was achieved.

The results of electrochemical-impedance spectroscopy (EIS) scanned on the carbon-steel sample immersed into the simulated brine saturated with CO_2 with and without the inhibitor in flow conditions are shown in Figures 7 and 8. In Table 6, experimental data adjusted with the equivalent circuits are shown.

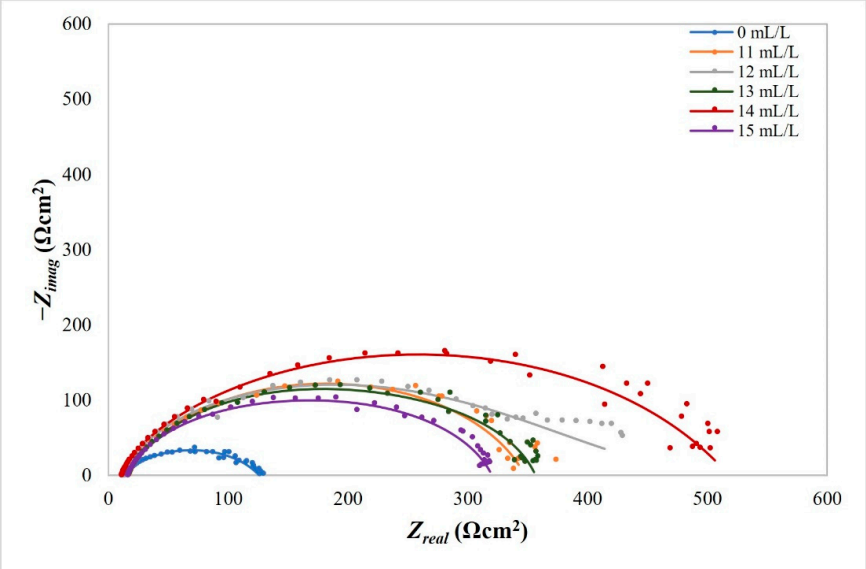

Figure 7. Nyquist plot scanned on the carbon-steel sample in the simulated brine saturated with CO_2 with and without the inhibitor in flow conditions (Adapted from [24]).

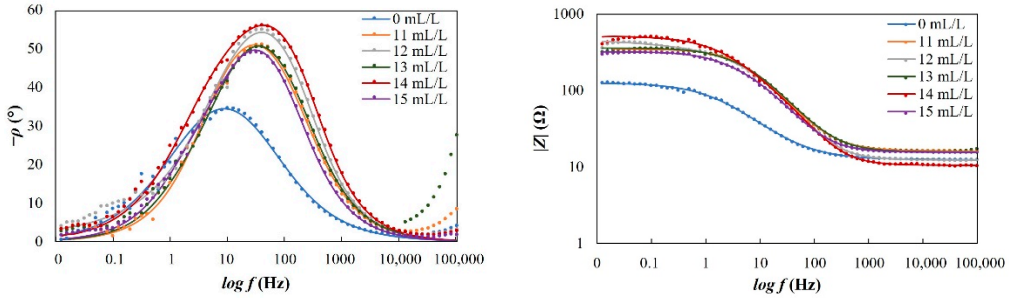

Figure 8. Bode plots scanned on the carbon-steel sample in the simulated brine saturated with CO_2 with and without the inhibitor in flow conditions (Adapted from [24]).

Table 6. Electrochemical parameters determined from Nyquist and Bode plots scanned on the carbon-steel sample in the simulated brine saturated with CO_2 with and without the inhibitor in flow conditions (Adapted from [24]).

γ (mL/L)	0	11	12	13	14	15
R_{el} (Ω)	12.31	15.94	12.24	15.61	10.43	15.43
Q_{dl} ($\mu\Omega^{-1}$ s^n)	1840	200	130	130	180	210
n_1	0.68	0.81	0.87	0.88	0.82	0.84
R_p (Ω)	113.68	331.43	340.74	471.10	508.16	304.61
Q_{inh} ($\mu\Omega^{-1}$ s^n)	-	-	610	220	48.3	120
n_2	-	-	0.32	0.61	0.89	0.80
R_{po} (Ω)	-	-	63.03	220.94	2,248.18	803.25
IE (%)		65.70	66.64	75.87	77.63	62.68

The same as in static conditions, the increase in the inhibitor concentration in flow conditions increases the diameters of Nyquist semicircles, the phase angle and impedance module (Figures 7 and 8). From Table 6, it can be seen that the increase in the inhibitor concentration leads to an increase in the charge-transfer resistance. Although the inhibitor efficiency increases with the increase in inhibitor concentration, the highest efficiency of 77.63% was achieved at 14 mL/L.

Comparisons of inhibitor efficiency due to different testing conditions are shown in Figures 9 and 10. The comparisons are divided by electrochemical method: Figure 9 shows the inhibitor efficiency calculated from the results of the potentiodynamic method and Figure 10 the results of the EIS method.

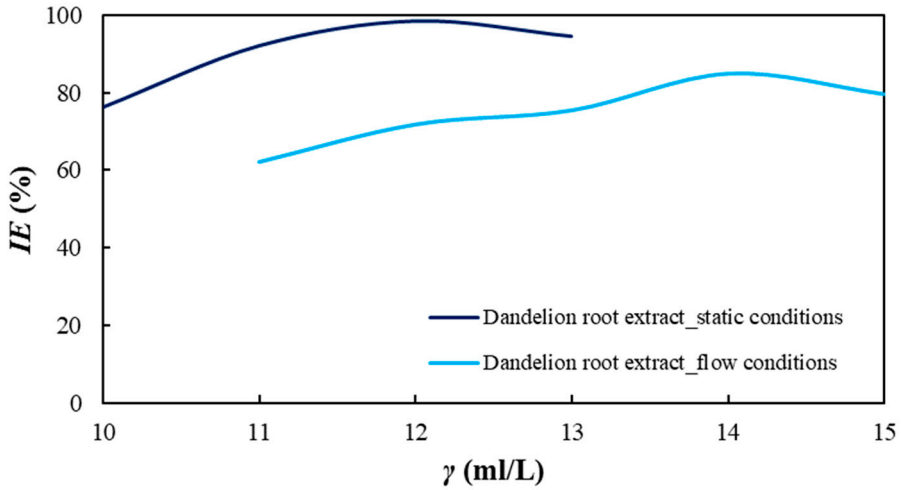

Figure 9. The inhibitor efficiency comparison determined from polarization curves scanned on the carbon-steel sample in the simulated brine saturated with CO_2 (Adapted from [24]).

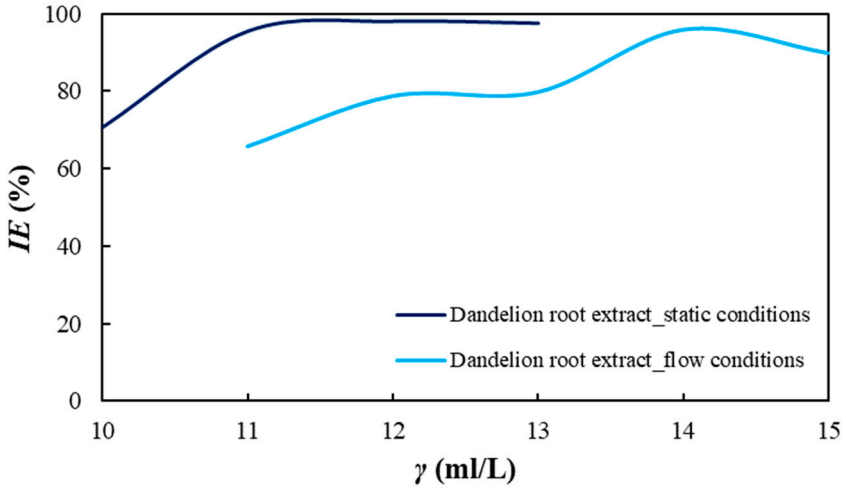

Figure 10. The inhibitor efficiency comparison determined from EIS scanned on the carbon-steel sample in the simulated brine saturated with CO_2 (Adapted from [24]).

As can be seen from Figures 9 and 10, dandelion-root extract achieved higher inhibition efficiency in static conditions and at lower inhibitor concentration.

3.2. SEM and FTIR

SEM analysis of the carbon-steel sample immersed into the uninhibited simulated brine is shown in Figure 11a and the analysis of the carbon-steel sample immersed into the solution inhibited with 12 mL/L of dandelion-root extract is shown in Figure 11b. The carbon-steel sample was immersed in the solutions for 4 h.

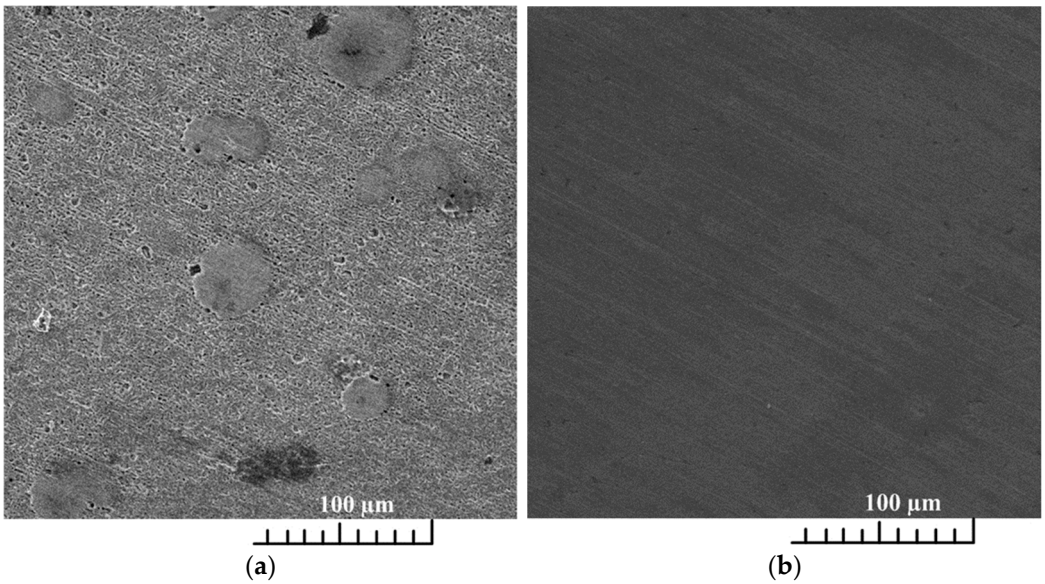

Figure 11. SEM scan of the carbon-steel sample after 4 h in the simulated brine saturated with CO_2 (**a**) without the extract and (**b**) with 12 mL/L of the extract (Adapted from [24]).

From Figure 11a, it can be seen that corrosion products are being formed on the steel surface. According to the conducted research, these products could be ferrous carbonate ($FeCO_3$), iron carbide (Fe_3C) and iron oxides [29]. From Figure 11b, the formation of a compact inhibitor film on the steel surface can be seen, which confirms the results of the conducted electrochemical measurements, which indicated that dandelion-root extract acts as a corrosion inhibitor.

A comparison of the FTIR analysis of dandelion-root extract and the analysis of the carbon-steel sample immersed into the solution inhibited with 12 mL/L of dandelion-root extract is shown in Figure 12. For this analysis, immersion of the carbon-steel sample also lasted for 4 h.

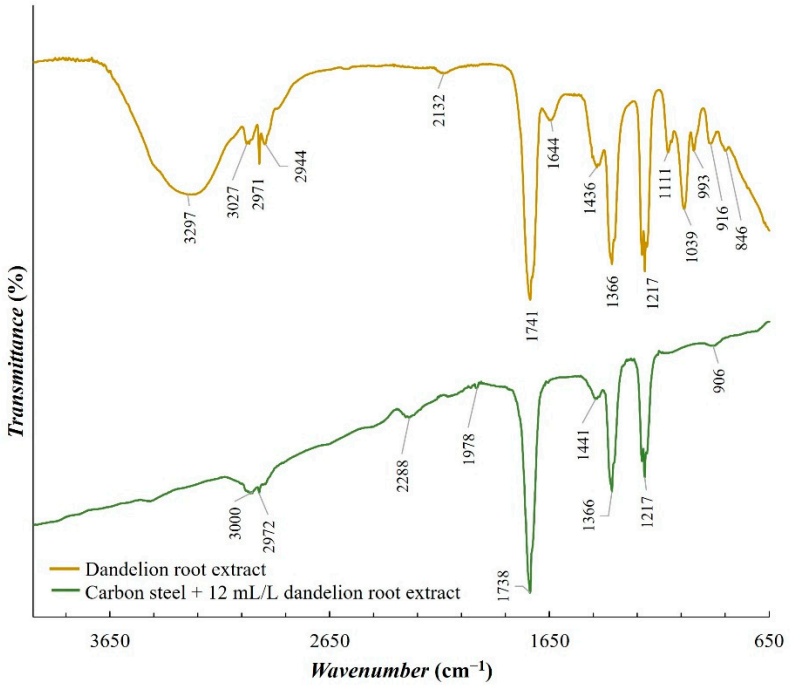

Figure 12. FTIR spectra of dandelion-root extract and the carbon-steel sample after 4 h of immersion in the simulated brine saturated with CO_2 with 12 mL/L of the extract (Adapted from [24]).

From the comparison of dandelion-root extract and the carbon-steel-sample surface after 4 h of immersion in the simulated brine saturated with CO_2 and 12 mL/L of the extract (Figure 12), the extract's adsorption on the steel surface can be observed. IR bands at 1217 cm^{-1}, 1366 cm^{-1} and 1741 cm^{-1} are related to C-N, C-C and C=O vibrations, respectively. Those three groups are the dominant functional groups in dandelion-root extract. Additionally, C-O (1039 cm^{-1}), C-H (2944–3027 cm^{-1}) and O-H (3297 cm^{-1}) functional groups are present [30]. The FTIR spectra of the inhibitor film on the steel sample surface compared with the FTIR spectra of dandelion-root extract shows the same dominant functional groups, where the C=O group stood out the most. It indicates that the extract was adsorbed on the sample surface through these groups of active components. With the results of FTIR spectra analysis, the adsorption of the extract on the steel sample surface is also confirmed as it was shown by electrochemical measurements.

3.3. Biodegradability and Toxicity

In Table 7, the chemical properties and toxicity of dandelion-root extract are given. Parameter EC_{50} represents the volume fraction of the sample that causes a 50% reduction of the light emitted by bacteria. Toxic units (*TUs*) are calculated according to the Equation (4) [31]. This units represent relative toxicity, and a higher value of *TU* indicates a higher toxicity of the tested sample.

$$TU(\%) = \frac{1}{EC_{50}} \times 100 \quad (4)$$

Table 7. Chemical properties and toxicity of dandelion-root extract (Adapted from [24]).

Parameter	Dandelion-Root Extract (γ = 12 mL/L)
BOD_5 (mgO_2/L)	10,359
COD (mgO_2/L)	10,790
BOD_5/COD	0.96
EC_{50} (%)	42.07
TU (%)	2.38

The *COD* value indicates a high concentration of organic substances in the extract. The BOD_5 and *COD* ratio almost equals 1 (0.96), which indicates dandelion-root extract's high biodegradability [31]. The toxic unit of dandelion-root extract is 2.38. According to Ledda et al., for a value of toxic unit between 1–40%, the compound is categorized as toxic [32]. Even though the tested extract falls into the category of toxic compounds, the TU value of 2.38, which is close to the lower range limit, which reflects the extract's mild toxicity. The TU value, in this case, primarily depends on the applied concentration and the presence of organic substances.

4. Conclusions

Dandelion-root extract was analyzed in static and flow conditions in a simulated brine solution saturated with CO_2 by potentiodynamic polarization and electrochemical-impedance spectroscopy. The extract proved to be an effective corrosion inhibitor in both conditions. In static conditions, the highest inhibitor efficiency of 98.37% was achieved at a concentration of 12 mL/L of the inhibitor, but in flow conditions, the efficiency was 82.8% at a concentration of 14 mL/L. The extract behaved as a mixed-type inhibitor. An SEM scan of the carbon-steel-sample surface showed a uniform surface compared to the steel sample surface from the uninhibited solution. This indicates the adsorption of the inhibitor onto the surface of the examined steel sample. Regarding the FTIR scans, dandelion-root extract was adsorbed to the steel sample surface by C-N (1217 cm^{-1}), C-C (1366 cm^{-1}) and C=O (1738 cm^{-1}) functional groups. The conducted biodegradability and toxicity analyses showed that dandelion-root extract is almost completely biodegradable (0.96) and with a value of toxicity of 2.38, from which it can be concluded that this extract is environmentally acceptable. Future research should be aimed at testing the inhibition efficiency of dandelion-root extract in systems in which, in addition to brine and dissolved CO_2, there are also hydrocarbon components. Additionally, in order to simulate as realistic conditions as possible, future research should be conducted under conditions of different high temperatures and pressures.

Author Contributions: Conceptualization, K.Ž., L.H.; G.B. and K.S.; methodology, G.B.; formal analysis, K.Ž., G.B., L.H. and K.S.; investigation, K.Ž.; resources, G.B. and L.H.; writing—original draft preparation, K.Ž. and L.H; writing—review and editing, K.Ž., L.H.; G.B. and K.S.; visualization, K.Ž.; supervision, G.B., L.H. and K.S; project administration, G.B. and L.H.; funding acquisition, K.S. All authors have read and agreed to the published version of the manuscript.

Funding: This research was funded by the institutional project *Circular Economy in the Petroleum Industry-KENI*, Faculty of Mining, Geology and Petroleum Engineering, University of Zagreb, Croatia.

Institutional Review Board Statement: Not applicable.

Informed Consent Statement: Not applicable.

Data Availability Statement: The data presented in this study are openly available in https://repozitorij.rgn.unizg.hr/islandora/object/rgn:1882 (accessed on 12 January 2022).

Conflicts of Interest: The authors declare no conflict of interest. The funders had no role in the design of the study; in the collection, analyses, or interpretation of data; in the writing of the manuscript, or in the decision to publish the results.

References

1. Nesic, S.; Wang, S.; Cai, J.; Xiao, Y. *Integrated CO_2 Corrosion-Multiphase Flow Model, Paper Presented at the SPE International Symposium on Oilfield Corrosion*; OnePetro: Aberdeen, UK, 2004.
2. Prasad, A.R.; Kunyankandy, A.; Joseph, A. Corrosion Inhibition in Oil and Gas Industry: Economic Considerations. In *Corrosion Inhibitors in Oil and Gas Industry*, 1st ed.; Saji, V.S., Umoren, S.A., Eds.; Wiley-VCH Verlag GmbH & Co KGaA: Weinheim, Germany, 2020; pp. 135–150.
3. Koch, G.; Varney, J.; Thompson, N.; Moghissi, O.; Gould, M.; Payer, J. *International Measures and Prevention, Application and Economics of Corrosion Technologies Study*; Report; NACE International: Houston, TX, USA, 2016.
4. Palou, R.M.; Olivares-Xomelt, O.; Likhanova, N.V. Environmentally Friendly Corrosion Inhibitors. In *Developments in Corrosion Protection*; Aliofkhazraei, M., Ed.; IntechOpen: London, UK, 2014; pp. 431–465.
5. Goni, L.K.M.O.; Mazumder, M.A.J. Green Corrosion Inhibitors. In *Corrosion Inhibitors*; Singh, A., Ed.; IntechOpen: London, UK, 2019.
6. Montemor, M.F. Fostering Green Inhibitors for Corrosion Prevention. In *Active Protective Coatings*; Hughes, A., Mol, J., Zheludkevich, M., Buchheit, R., Eds.; Springer Series in Materials Science; Springer: Dordrecht, The Netherlands, 2016; Volume 233, pp. 107–137.
7. Shehata, O.S.; Korshed, L.A.; Attia, A. Green Corrosion Inhibitors, Past, Present and Future. In *Corrosion Inhibitors, Principles and Recent Applications*; Aliofkhazraei, M., Ed.; IntechOpen: London, UK, 2018; pp. 121–142.
8. Popoola, L.T. Organic green corrosion inhibitors (OGCIs): A critical review. *Corros. Rev.* **2019**, *37*, 71–102. [CrossRef]
9. Fazal, B.R.; Becker, T.; Kinsella, B.; Lepkova, K. A review of plant extracts as green corrosion inhibitors for CO_2 corrosion of carbon steel. *npj Mater. Degrad.* **2022**, *6*, 5. [CrossRef]
10. Qiang, Y.; Zhang, S.; Tan, B.; Chen, S. Evaluation of Ginkgo leaf extract as an eco-friendly corrosion inhibitor of X70 steel in HCl solution. *Corros. Sci.* **2018**, *133*, 6–16. [CrossRef]
11. Saxena, A.; Prasad, D.; Haldhar, R.; Singh, G.; Kumar, A. Use of *Saraca ashoka* extract as green corrosion inhibitor for mild steel in 0.5 M H_2SO_4. *J. Mol. Liq.* **2018**, *258*, 89–97. [CrossRef]
12. Saxena, A.; Prasad, D.; Haldhar, R.; Singh, G.; Kumar, A. Use of *Sida cordifolia* extract as green corrosion inhibitor for mild steel in 0.5 M H_2SO_4. *J. Environ. Chem. Eng.* **2018**, *6*, 694–700. [CrossRef]
13. Ugi, B.U.; Obeten, M.E.; Magu, T.O. Phytochemical constituents of Taraxacum officinale leaves as eco-friendly and nontoxic organic inhibitors for stainless steel corrosion in 0.2 M HCl acid Medium. *Int. J. Chem. Sci.* **2018**, *2*, 35–43.
14. Dehghani, A.; Blahlakeh, G.; Ramezanzadeh, B.; Ramezanzadeh, M. A combined experimental and theoretical study of green corrosion inhibition of mild steel in HCl solution by aqueous *Citrullus lanatus* fruit (CLF) extract. *J. Mol. Liq.* **2019**, *279*, 603–624. [CrossRef]
15. Khan, M.; Abdullah, M.M.S.; Mahmood, A.; Al-Mayouf, A.M.; Alkhathlan, H.Z. Evaluation of *Matricaria aurea* Extracts as Effective Anti-Corrosive Agent for Mild Steel in 1.0 M HCl and Isolation of Their Active Ingredients. *Sustainability* **2019**, *11*, 7174. [CrossRef]
16. Saeed, M.T.; Saleem, M.; Niyazi, A.H.; Al-Shamrani, F.A.; Jazzar, N.A.; Ali, M. Carrot (*Daucus Carota* L.) Peels Extract as an Herbal Corrosion Inhibitor for Mild Steel in 1M HCl Solution. *Mod. Appl. Sci.* **2020**, *14*, 97–112. [CrossRef]
17. Mauro, A.C.; Ribeiro, B.D.; Garrett, R.; Borges, R.M.; da Silva, T.U.; de Paula Machado, S.; de Araujo, J.R.; de Oliveira Massafra, S.; de Oliveira Junior, F.O.R.; D'Elia, E. *Ziziphus joazeiro* Stem Bark Extract as a Green Corrosion Inhibitor for Mild Steel in Acid Medium. *Processes* **2021**, *9*, 1323. [CrossRef]
18. Gapsari, F.; Darmadi, D.B.; Setyarini, P.H.; Izzuddin, H.; Madurani, K.A.; Tanji, A.; Hermawan, H. *Nephelium lappaceum* Extract as an Organic Inhibitor to Control the Corrosion of Carbon Steel Weldment in the Acidic Environment. *Sustainability* **2021**, *13*, 12135. [CrossRef]
19. Pustaj, G.; Kapor, F.; Jakovljević, S. Carbon dioxide corrosion of carbon steel and corrosion inhibition by natural olive leaf extract: Die Kohlendioxid-Korrosion von Kohlenstoffstahl und die Korrosionshemmung durch natürlichen Olivenblattextrakt. *Mater. Werkst.* **2017**, *48*, 122–138. [CrossRef]
20. Devikala, S.; Kamaraj, P.; Arthanareeswari, M.; Patel, M.B. Green corrosion inhibition of mild steel by aqueous *Allium sativum* extract in 3.5% NaCl. *Mater. Today Proc.* **2019**, *14*, 580–589. [CrossRef]
21. Devikala, S.; Kamaraj, P.; Arthanareeswari, M.; Patel, M.B. Green corrosion inhibition of mild steel by *Asafoetida extract* in 3.5% NaCl. *Mater. Today Proc.* **2019**, *14*, 590–601. [CrossRef]
22. Barbouchi, M.; Benzidia, B.; Aouidate, A.; Ghaleb, A.; El Idrissi, M.; Choukrad, M. Theoretical modeling and experimental studies of Terebinth extracts as green corrosion inhibitor for iron in 3% NaCl medium. *J. King Saud Univ.–Sci.* **2020**, *32*, 2995–3004. [CrossRef]
23. Žbulj, K.; Bilić, G.; Hrnčević, L.; Simon, K. Potential of using plant extracts as green corrosion inhibitors in the petroleum industry. *Rud.-Geološko-Naft. Zb.* **2021**, *36*, 131–139. [CrossRef]
24. Žbulj, K. Extracts of Selected Plants as Steel Corrosion Inhibitors in Hydrocarbon Production and Transportation Systems. Doctoral Thesis, Faculty of Mining, Geology and Petroleum Engineering, University of Zagreb, Zagreb, Croatia, 7 December 2021.
25. Sastri, V.S. *Green Corrosion Inhibitors: Theory and Practice*; John Wiley & Sons, Inc.: Hoboken, NJ, USA, 2011.
26. Amin, M.A.; Khaled, K.F.; Fadl-Allah, S.A. Testing validity of the Tafel extrapolation method for monitoring corrosion of cold rolled steel in HCl solutions—Experimental and theoretical studies. *Corros. Sci.* **2010**, *52*, 140–151. [CrossRef]

27. Boukamp, B.A. *Equivalent Circuit*; University of Twente: Enschede, The Netherlands, 1989.
28. Majd, M.T.; Ramezanzadeh, M.; Bahlakeh, G.; Ramezanzadeh, B. Steel corrosion lowering in front of the saline solution by a nitrogen-rich source of green inhibitors: Detailed surface, electrochemical and computational studies. *Constr. Build. Mater.* **2020**, *254*, 119266. [CrossRef]
29. Kinsella, B.; Tan, Y.J.; Bailey, S. Electrochemical Impedance Spectroscopy and Surface Characterization Techniques to Study Carbon Dioxide Corrosion Product Scales. *Corrosion* **1998**, *54*, 835–842. [CrossRef]
30. Pavia, D.L.; Lampman, G.M.; Kriz, G.S. *Introduction to Spectroscopy*, 5th ed.; Cengage Learning: Stamford, CT, USA, 2015.
31. Samudro, G.; Mangkoedihardjo, S. Review on BOD, COD and BOD/COD ratio: A triangle zone for toxic, biodegradable and stable levels. *Int. J. Acad. Res.* **2010**, *2*, 235–239.
32. Ledda, C.; Rapisarda, V.; Bracci, M.; Proietti, L.; Zuccarello, M.; Fallico, R.; Fiore, M.; Ferrante, M. Professional exposure to basaltic rock dust: Assessment by the Vibrio fischeri ecotoxicological test. *J. Occup. Med. Toxicol.* **2013**, *8*, 23. [CrossRef] [PubMed]